

Li Cai · Jianguo Wang · Mi Zhou ·
Jinxin Cao · Yadong Fan

Rocket-Triggered Lightning

The Development of Physical Process
and Effect of Lightning Discharge

 Springer

Rocket-Triggered Lightning

Li Cai · Jianguo Wang · Mi Zhou · Jinxin Cao ·
Yadong Fan

Rocket-Triggered Lightning

The Development of Physical Process
and Effect of Lightning Discharge

Li Cai
Wuhan University
Wuhan, Hubei, China

Jianguo Wang
Wuhan University
Wuhan, Hubei, China

Mi Zhou
Wuhan University
Wuhan, Hubei, China

Jinxin Cao
Wuhan University
Wuhan, Hubei, China

Yadong Fan
Wuhan University
Wuhan, Hubei, China

ISBN 978-981-97-2346-1 ISBN 978-981-97-2347-8 (eBook)
<https://doi.org/10.1007/978-981-97-2347-8>

© The Editor(s) (if applicable) and The Author(s), under exclusive license to Springer Nature Singapore Pte Ltd. 2024

This work is subject to copyright. All rights are solely and exclusively licensed by the Publisher, whether the whole or part of the material is concerned, specifically the rights of translation, reprinting, reuse of illustrations, recitation, broadcasting, reproduction on microfilms or in any other physical way, and transmission or information storage and retrieval, electronic adaptation, computer software, or by similar or dissimilar methodology now known or hereafter developed.

The use of general descriptive names, registered names, trademarks, service marks, etc. in this publication does not imply, even in the absence of a specific statement, that such names are exempt from the relevant protective laws and regulations and therefore free for general use.

The publisher, the authors and the editors are safe to assume that the advice and information in this book are believed to be true and accurate at the date of publication. Neither the publisher nor the authors or the editors give a warranty, expressed or implied, with respect to the material contained herein or for any errors or omissions that may have been made. The publisher remains neutral with regard to jurisdictional claims in published maps and institutional affiliations.

This Springer imprint is published by the registered company Springer Nature Singapore Pte Ltd. The registered company address is: 152 Beach Road, #21-01/04 Gateway East, Singapore 189721, Singapore

If disposing of this product, please recycle the paper.

Contents

| | | |
|----------|--|-----------|
| 1 | History of Rocket Triggered Lightning | 1 |
| 1.1 | Introduction | 1 |
| 1.2 | Rocket Triggered Lightning Techniques | 3 |
| 1.3 | Comprehensive Observation of Rocket Triggered Lightning at Different Development Stages | 8 |
| 1.3.1 | Dart Leader Stage | 8 |
| 1.3.2 | Initial Discharge Stage | 11 |
| 1.3.3 | Return Stroke Stage | 13 |
| 1.3.4 | Continuous Current Stage | 14 |
| | References | 16 |
| 2 | Characteristics of Lightning Current of Rocket-Triggered Lightning | 19 |
| 2.1 | IS Currents | 19 |
| 2.1.1 | Parameters of IS Current | 19 |
| 2.1.2 | Characteristics of Initial Stage Current Accompanied by no Return Stroke | 23 |
| 2.1.3 | Characteristics of Initial Stage Current Accompanied by Return Strokes | 24 |
| 2.1.4 | Discharge Mode of Initial Stage of Flashes with and Without Return Strokes in Rocket-Triggered Lightning | 26 |
| 2.2 | RS Currents | 30 |
| 2.2.1 | Parameters of RS Current | 30 |
| 2.2.2 | Simulation of RS Currents | 34 |
| 2.2.3 | Correlations Between RS Current Parameters | 35 |
| 2.3 | Continuing Current and M Component Currents | 38 |
| 2.3.1 | Characteristics of Continuing Current Waveform with Duration Less Than 10 ms | 38 |
| 2.3.2 | Characteristics of Continuing Current Waveform with Duration More Than 10 ms | 42 |

| | | |
|----------|--|------------|
| 2.3.3 | Characteristics of M Component Parameters | 47 |
| 2.3.4 | “Exclusion Zone” in M Component Waveform Parameters | 52 |
| 2.4 | Summary | 56 |
| 2.4.1 | IS Currents | 56 |
| 2.4.2 | RS Currents | 56 |
| 2.4.3 | Continuing Current and M Component Currents | 57 |
| | References | 57 |
| 3 | Characteristics of Magnetic Field of Rocket-Triggered Lightning | 59 |
| 3.1 | Magnetic Sensor and Definitions of Magnetic Field Waveform Parameters | 59 |
| 3.2 | Parameters of Magnetic Field at Different Distances | 62 |
| 3.2.1 | Magnetic Field at 18 m | 62 |
| 3.2.2 | Magnetic Field at 130 m | 63 |
| 3.2.3 | Magnetic Field at 1550 m | 64 |
| 3.3 | Influence of Distance on Characteristic Parameters of Magnetic Field | 66 |
| 3.4 | Measurement of Return Stroke Current with Magnetic Sensor | 69 |
| 3.4.1 | Method and Theory | 69 |
| 3.4.2 | Results and Analysis | 73 |
| 3.5 | Summary | 76 |
| | References | 77 |
| 4 | Characteristics of Electric Field of Rocket-Triggered Lightning | 79 |
| 4.1 | Electric Field Sensor and Definitions of Electric Field Waveform Parameters | 80 |
| 4.2 | Parameters of Electric Field at Close Distances | 82 |
| 4.2.1 | Electric Field at 58 m | 83 |
| 4.2.2 | Electric Field at 90 m | 89 |
| 4.3 | Parameters of Electric Field at Far Distances | 93 |
| 4.4 | Comparison Between Far Electric Field Waveforms of Triggered Return Strokes and Natural Return Strokes from the Same Thunderstorms | 99 |
| 4.5 | Summary | 109 |
| | References | 110 |
| 5 | Progressing Characteristics of Dart Leaders in Rocket Triggered Lightning Flashes | 113 |
| 5.1 | Bidirectional Leader Development in Rocket-Triggered Lightning Flashes | 113 |
| 5.1.1 | Background | 113 |

- 5.1.2 Case Presentation 114
- 5.1.3 Discussion 118
- 5.2 Leader-Chasing Behavior in Rocket Triggered Lightning Flashes 120
 - 5.2.1 Background 120
 - 5.2.2 Case I Presentation 121
 - 5.2.3 Case II Presentation 124
 - 5.2.4 Discussion 127
- 5.3 Attempted Leaders Development in a Rocket Triggered Lightning Flashes 130
 - 5.3.1 Background 130
 - 5.3.2 Data Presentation 132
 - 5.3.3 Progressing Characteristics of Leaders in Group Path 1 and Path 2 135
 - 5.3.4 Progressing Characteristics of Leaders in Group Path 3 137
 - 5.3.5 Discussion 140
- 5.4 Observation of Five Types of Leaders Contained in a Negative Triggered Lightning 144
 - 5.4.1 Background 144
 - 5.4.2 Five Types of Leader 146
 - 5.4.3 Upward Positive Dart Leader 148
 - 5.4.4 Bidirectional Leader 150
 - 5.4.5 Dart Stepped Leader 150
 - 5.4.6 Propagation Speeds 153
 - 5.4.7 Discussion 155
- 5.5 Summary 158
- References 159
- 6 Acoustic Observation of Rocket Triggered Lightning Flashes 161**
 - 6.1 Characteristics of Acoustic Response from Simulated Impulsive Lightning Current Discharge 161
 - 6.1.1 Background 161
 - 6.1.2 Instruments and Method 163
 - 6.1.3 Acoustic Response of Impulsive Discharge 164
 - 6.1.4 Characteristics of Acoustic Parameters 166
 - 6.1.5 Acoustic Response of Current Discharge with Subsequent Peaks 169
 - 6.2 Triggered Lightning Acoustic Response with Return Stroke Current at 90 m and 130 m 173
 - 6.2.1 Background 173
 - 6.2.2 Complete Acoustic Waveforms of RS Process 175
 - 6.2.3 Acoustic N-shape Waves of RS Process 177
 - 6.2.4 Low Frequency Acoustic Waveforms of RS Process 183
 - 6.2.5 Discussion 185
 - 6.3 Triggered Lightning Acoustic Signature and Location 188

- 6.3.1 Background 188
- 6.3.2 Data Analysis 189
- 6.3.3 First Arrival Acoustic N-waves Characterization 192
- 6.3.4 Acoustic Low Frequency Waves Characterization 194
- 6.3.5 Acoustic Characterization of Other Discharge Processes 196
- 6.3.6 Acoustic Radiations Location 198
- 6.3.7 Discussion 199
- 6.4 Summary 201
- References 203
- 7 Optical Progressing and Electric Field Change Characteristics of Altitude-Triggered Lightning Flash 205**
 - 7.1 Background 205
 - 7.2 Characteristics of the Bidirectional Leader-Mini Return Stroke 207
 - 7.3 Characteristics of the Initial Continuous Current Pulses 209
 - 7.4 Characteristics of the Dart Leader-Return Stroke 211
 - 7.5 Characteristics of the M Components 218
 - 7.6 Modeling of Dart Leader Development in an Altitude-Triggered Lightning Flash 220
 - 7.6.1 Normal Dart Leader Process 221
 - 7.6.2 Dart Leader Process with Chasing Leader 227
 - 7.6.3 Dart Leader Process with Bidirectional Leader 229
 - 7.6.4 Discussion 233
 - 7.6.5 Modeling of Attempted Leaders in an Altitude-Triggered Lightning Flash 236
 - 7.7 Summary 247
 - References 248
- 8 Development Characteristics of Triggered Lightning with Fast Initial Continuous Current Pulses and Two Grounding Points 251**
 - 8.1 Background 251
 - 8.2 Data 252
 - 8.3 Characteristics of the IS, RS1 and RS2 at Grounding Point 1 255
 - 8.4 The Process of RS3 Forming a New Grounding Point 261
 - 8.5 Discussion 265
 - 8.6 Summary 269
 - References 270
- 9 Differences Between Triggered Lightning Striking to Ground and Distribution Line 273**
 - 9.1 Background 273
 - 9.2 Differences Between Currents of Triggered Lightning Striking to Distribution Line and Ground 274
 - 9.2.1 Characteristics of the IS Current Waveforms 274

- 9.2.2 Characteristics of the RS Current Waveforms 277
- 9.2.3 Discussion 279
- 9.3 Differences Between the Close Magnetic Field of Triggered
Lightning Striking to Distribution Line and Ground 282
- 9.4 Differences Between the Close Electric Field of Triggered
Lightning Striking to Distribution Line and Ground 285
- 9.5 Differences Between the Far Electric Field of Triggered
Lightning Striking to Distribution Line and Ground 289
- 9.6 Discussion 293
- 9.7 Summary 294
- References 296

Chapter 1

History of Rocket Triggered Lightning



1.1 Introduction

The scientific exploration of lightning has always been the concern of many scholars, but due to the instantaneity and randomness of lightning, it is difficult to make a stable scientific observation of lightning. In the mid-twentieth century, the development of artificial lightning trigger technology, that is, by launching small rockets with metal wires into a lightning cloud, lightning can occur at a predicted time and place, providing conditions for direct measurement of lightning currents and electromagnetic fields.

The first documented triggered lightning, with rockets carrying the wire, was illustrated in the 1960s. It was implemented on a boat at sea in Florida [1]. Since 1973, this technology has been improved on land by a number of countries, including France, Japan, China, and Brazil, as shown in Table 1.1. The lightning team from the International Center for Lightning Research and Testing (ICLRT) in Florida also conducted an amount of experiments with rocket-wire artificially triggered lightning. Rakov and Uman et al. [2] had conducted a comprehensive summary and review of the research results of the artificial triggered lightning tests in the United States. It has made great contributions to the measurement of lightning discharge parameters, discharge physical process, electromagnetic radiation effect and theoretical simulation.

Since 1989, China had performed triggered-lightning experiments in Jiangxi, Gansu, Beijing, Guangdong and Shandong, respectively. In particular, in the past 10 years, two teams from the Chinese Academy of Meteorological Sciences and the Institute of Atmospheric Physics have been continuously conducting experiments on artificially induced lightning in Guangdong Province [3] (GCOELD) and Shandong Province [4] (SHATLE), respectively. These experiments not only deepen our understanding of the physical characteristics of lightning, but also play an important role in studying and testing the mechanism of lightning strike and evaluating the

Table 1.1 An overview of major triggered-lightning programs

| Experimental site | Height above sea level, m | Years of operation | Wire material | Location of wire spool |
|---|---------------------------|--------------------|-----------------|------------------------|
| Saint Prival d'Allier, France | 1100 | 1973–1996 | Steel or copper | Ground or rocket |
| Kahokugata, Hokuriku coast, Japan | 0 | 1977–1985 | Steel | Ground |
| Langmuir Laboratory, New Mexico, USA | 3230 | 1979–present | Steel | Ground |
| KSC, Florida, USA | 0 | 1983–1991 | Copper | Rocket |
| Okushishiku, Japan | 930 | 1986–1998 | Steel | Ground or rocket |
| Fort McClellan, Alabama, USA | 190 | 1991–1995 | Copper | Rocket |
| Camp Blanding, Florida, USA | 5–20 | 1993–present | Copper | Rocket |
| Cachoeira Paulista, Brazil | 570 | 1993–present | Copper | Rocket |
| Four sites in northern and southeastern China | Various | 1989–1998 | Steel or copper | Ground or rocket |
| Chonghua, Guangdong, China | 80 | 2006–present | Copper | Rocket |
| Binzhou, Shandong, China | 3–20 | 2006–present | Copper | Rocket |

performance of lightning location system. Although the parameters related to lightning discharge have been analyzed and studied all over the world, in general, we still need to accumulate enough lightning discharge data in different areas to determine the lightning discharge mode and provide accurate lightning discharge parameters required for lightning protection work.

1.2 Rocket Triggered Lightning Techniques

The idea of manually triggering lightning by using a small rocket with metal wires trailing at the tail was proposed in 1958. In 1961, laboratory tests proved that static metal wire would not trigger discharge phenomenon in a certain intensity of environmental electric field, while fast moving metal wire would trigger discharge phenomenon in a certain intensity of environmental electric field. The first artificial triggering of lightning on the sea was achieved in 1967, and then the artificial triggering of lightning on the land by using the trailing wire of hail proof rocket was achieved in 1978.

The traditional method of manually triggered lightning, also known as the “classical method,” works by launching a small rocket at the bottom of a thunderstorm cloud with a metal wire trailing behind it, the end of which is eventually grounded by a current-measuring device or test target. In order to simulate the descending cascade leading process in natural lightning, the “aerial method” technology of artificially triggering lightning has been developed in recent years. Different from the “classical method”, the “altitude method” of the mine rocket drag lead is not the whole metal wire, the end is generally nylon wire or Kevlar fiber wire, so as to achieve the metal wire insulation to the ground.

As is shown in Fig. 1.1, when the lightning-leading rocket rises to a certain height, the electric field around the metal line is enhanced, and the positive polarity stepped leader begins to appear and develops steadily upward, thus the so-called “initial stage” begins. With the development of the upward positive stepped leader, the current flowing on the wire also gradually increases. When the current intensity and flow time reach a certain degree, the wire begins to fuse and be broken down and shine after about several hundred microseconds. The discharge channel conducts again, and the upward positive stepped leader further develops towards the cloud bottom. When the upward positive stepped leader enters the charge region, the initial continuous current stage begins, and the discharge activities continue in the channel created by the upward cascade leader. The initial continuous current lasts for about a few hundred milliseconds. After the “initial stage” is over, the current in the channel stops for about a few tens of milliseconds. At this point, the discharge channel becomes dim, which is called the residual channel. After the “initial stage” is over, one or more subsequent return strokes may occur in the residual channel from downward-going negative arrow leader propagation to ground, known as the dart leader/subsequent return stroke sequence.

The difference between the “altitude method” and the “classical method” mainly focuses on the initial continuous current stage before the start of the lightning discharge process. Figure 1.2 shows the development of the altitude method artificial lightning at this stage. When the rocket reaches a certain altitude, the upward positive stepped leader begins to develop upward, and about a few milliseconds later, the downward negative stepped leader begins to appear at the bottom of the metal section of the “dangling” rocket lead. When the downward negative stepped leader is developed to the ground, there will be an upward positive connection leader on

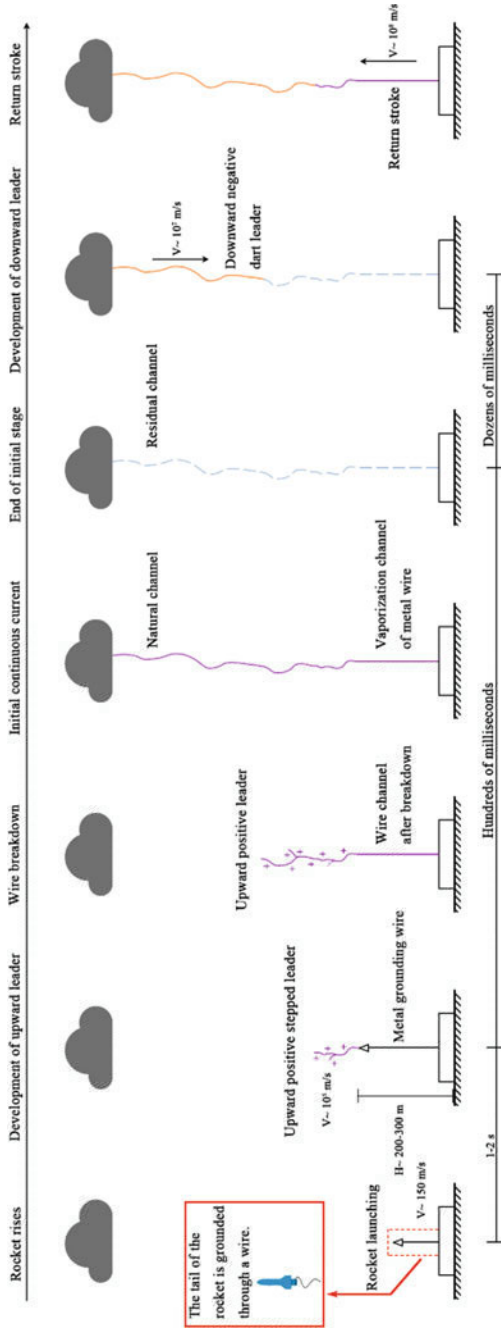


Fig. 1.1 The development of classical triggered lightning

the ground, and then the two leaders meet for the so-called “connection process”. After the connection of the two leads, there will be a “small return stroke” at the connection point that develops along the channel created by the downward negative cascade leader. The “small return stroke” will eventually break down the metal wire and reach the head position of the upward positive stepped leader. The initial continuous current phase begins when the upward positive stepped leader enters the negative charge zone. Since the channel from the bottom of the “suspended” metal wire to the ground is constructed by the downward negative stepped leader and the upward positive connection leader, the bottom of the artificially triggered lightning discharge channel of the “altitude method” is also a natural channel.

In the summer of 2018 and 2019, the Lightning Protection and Grounding Technology Center from Wuhan University conducted a rocket-triggered lightning experiment at Guangzhou Field Experiment Site for Lightning Research and Testing (GFESLRT, Guangdong Province, China). Chinese Academy of Meteorological Sciences and Guangdong Power Grid Scientific Research Institute also participated in this experiment. The new-generation rocket launch platform included fiber-optic isolation launch control device; dual fiber optic trigger ignition device; acoustic, optical, electrical and magnetic multi-parameter synchronous observation system, as well as insulation emission platform. Realizing the technical upgrade of lightning induction platform and the technical breakthrough of distribution line manual trigger lightning. For the first time, the observation data of lightning current, overvoltage along the line and acoustic, optical, electric and magnetic multi-parameter synchronization were obtained. On the one hand, lightning current is an important parameter reflecting the discharge process and lightning intensity, and on the other hand, the measurement of electromagnetic field is an important basis for lightning protection design and testing of ground flash return model.

The schematic diagram of the test site is shown in Fig. 1.3. There were two launchers in total, i.e., the ground launcher and the tower launcher. The grounding resistance of ground launcher is 6.7Ω . When lightning strikes to distribution line, the lightning current was first introduced into the current measuring equipment by the lightning rod, then flowed into one phase of the 10 kV distribution line (characteristic impedance is about several hundred ohms), and then flowed into the soil via the pole towers. The total length of the distribution line is 1.5 km, with a tower spacing of 70 m and a height of 10 m. The lightning current measurement equipment were a Rogowski coil and a coaxial shunt. The electric and magnetic field measurement at 130 m was set to be about 3.6 m above ground. And the electric and magnetic field measurement was also installed on the house roof (about 15 m high) 1.55 km away from the lightning triggering site. The analog current signals obtained by the measuring devices were transmitted to the control room via a fiber optic system. In addition, a high-speed camera (Phantom v2512 HS) also installed on the house roof was used to capture the images of the lightning flashes.

The Foshan Total Lightning Location System (FTLLS) 68–126 km away recorded the far RS electric field waveforms, the location distribution of the nine sub-stations (LSZ, 68.5 km; LPZ, 72.5 km; DTZ, 74.3 km; CCZ, 84.5 km; CCJ, 86.5 km; BNZ,

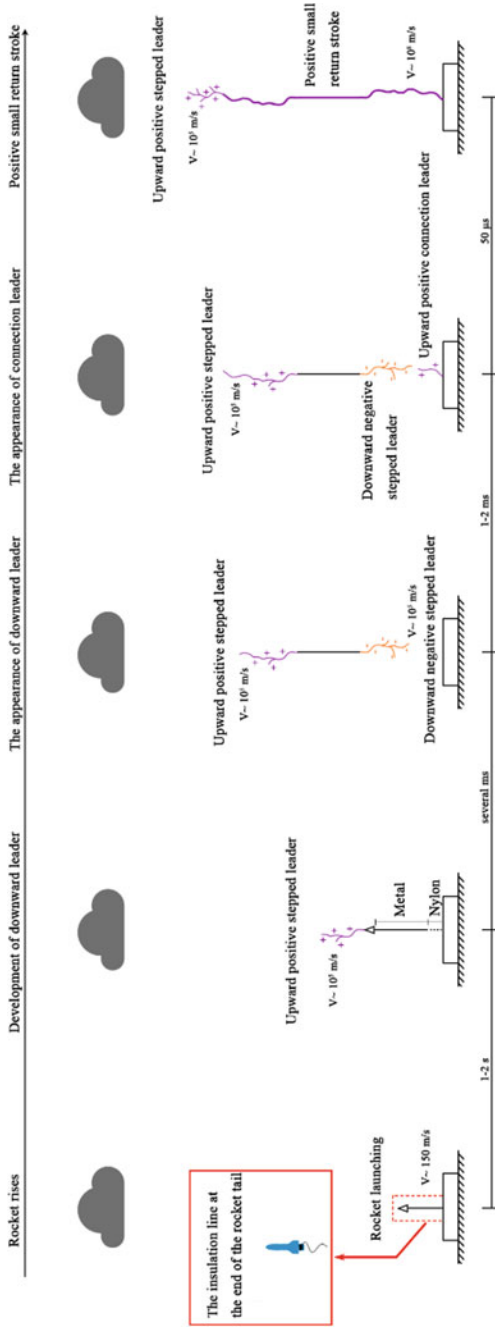


Fig. 1.2 The development of altitude-triggered lightning

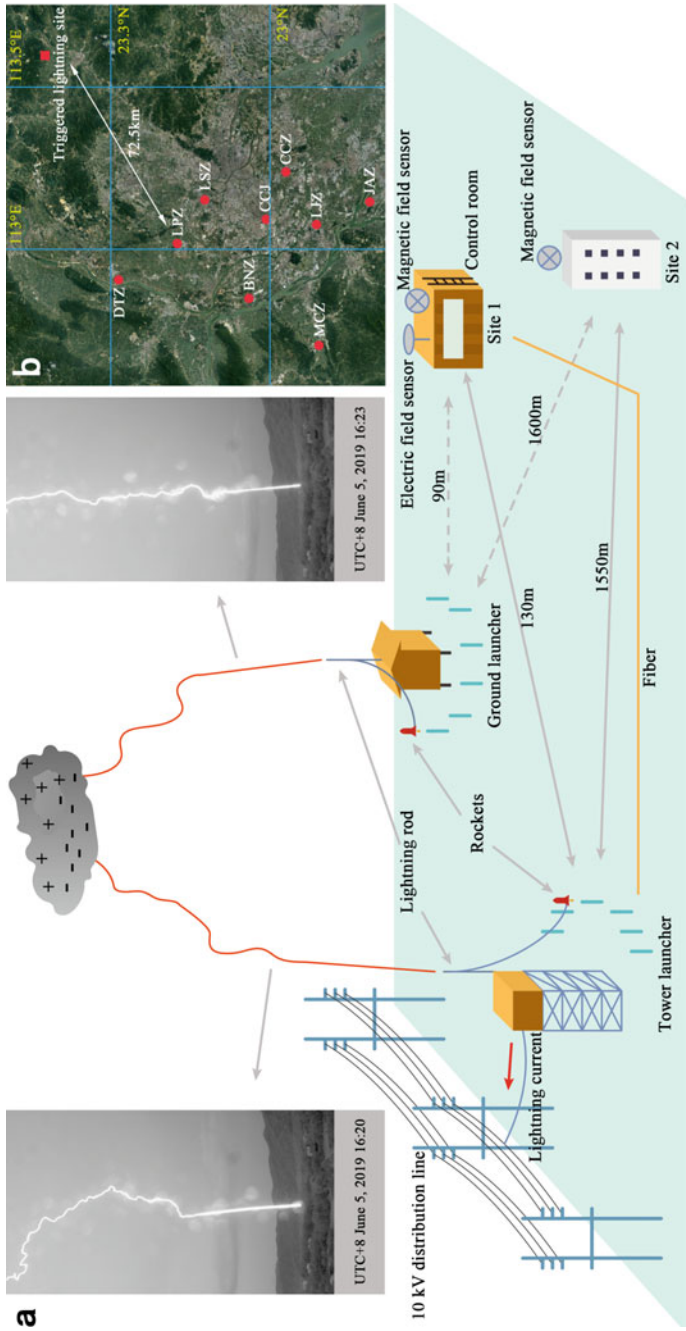


Fig. 1.3 Diagram of test site layout. **a** Schematic diagram of the test site. **b** Geographical location of the FTLLS sub-stations. The optical pictures of two RSS are also presented in (a)

Table 1.2 Information about triggered lightning flashes

| Triggering conditions | Number of launches | Number of successes (success rate) | Flashes with RSs (percentage of flashes with RSs) | Number of RSs | Multiplicity of RSs (AM) ^a |
|-----------------------|--------------------|------------------------------------|---|---------------|---------------------------------------|
| Ground | 47 | 34 (72%) | 22 (65%) | 106 | 4.8 |
| Distribution line | 35 | 26 (74%) | 20 (77%) | 120 | 6.0 |
| Total | 82 | 60 (73%) | 42 (70%) | 226 | 5.4 |

All flashes were negative and were triggered in the classic way

^aFor flashes with RSs. AM: arithmetic mean

99.8 km; LJZ, 100.8 km; JAZ, 112.4 km; MCZ, 125.7 km) of the FTLLS is shown in Fig. 1.3b, and their electric field sensors all have a sampling rate of 10 MHz.

During 2018–2019, a total of 82 launches were conducted, successfully triggering 60 lightning flashes, including 226 RSs. Detailed information is shown in Table 1.2. The success rate of our experiment is over 70%. About 70 percent of the flashes contained RSs, and the average number of RSs per flash is 5.4.

1.3 Comprehensive Observation of Rocket Triggered Lightning at Different Development Stages

Classical artificially triggered lightning mainly includes upward forward leader (UPL), initial continuous current (ICC), one or more downward arrow lead/return stroke processes, continuous current and M component processes. Among them, the upstream positive lead and the initial continuous current constitute the initial discharge stage (IS). The initial discharge process generally lasts from tens to hundreds of milliseconds. The current pulse superimposed on the initial continuous current IS called ICC pulse. Continuous current is usually defined as the lower amplitude current in the discharge channel immediately after the return stroke process, with a size of tens to hundreds of amperes and a duration of several milliseconds to several hundred milliseconds. The current pulse superimposed on the continuous current is called the M component.

1.3.1 Dart Leader Stage

Dart leader, unlike stepped leader developed in fresh air, tend to develop along residual channels constructed by stepped leader. The development process is continuous and intense, and the development rate is about 10^6 to 10^7 m/s. Forking is not easy in the development process of dart leader, and some dart leader may be transformed

into dart-stepped leader [5], that is, in the middle and late stage of development, the characteristics of stepped development, which may be caused by the gradual dissipation of residual channels and the continuous decline of electrical conductivity. Most of the observed dart leaders can successfully propagate to the ground and complete the connection process with the upstream leader to trigger the return stroke. The optical characteristics, propagation speed and other parameters of such dart leaders have been studied extensively.

With the increasing enrichment of observation means, some dart leader that failed to propagate successfully to ground have been observed successively. Rhodes et al. [6] reported this type of dart leader in 1994 and named them as attempted leads. In subsequent observations, the presence of attempted leads in lightning activity was speculated by using radio interferometers or measuring electric field changes. Shao et al. [7] observed four attempted leaders in negative ground lightning, and attempted leader were successfully observed in cloud-to-ground lightning, artificially triggered lightning and bipolar lightning. The use of high-speed cameras has made lightning observations more visible, but attempts are difficult to record with high-speed cameras because most attempts are short-lived and hidden in clouds.

Propagation speed is a basic characteristic parameter of the attempted leader. Shao et al. estimated the two-dimensional average propagation speed of the attempted leader by using the interferometer to be $7\text{--}10 \times 10^6$ m/s, which is five times of the case reported by Mardiana et al. Yoshida et al. calculated that the three-dimensional average propagation velocity of an attempted leader was 5.2×10^6 m/s by using the low-frequency sensor network. Wu et al. calculated that the overall propagation speed of an attempted leader was about 2.6×10^6 m/s by using the fast antenna lightning positioning array. Sun et al. calculated that the two-dimensional average propagation velocity of the attempted leader was $4\text{--}8 \times 10^6$ m/s by using the VHF lightning positioning system. By using high-speed cameras, Camops et al. reported a lightning with multiple attempted leader whose two-dimensional velocity was on the order of 10^6 m/s. With the help of high-speed cameras, Lyu et al. observed an attempted leader with a two-dimensional propagation velocity between 1.1×10^5 and 1.1×10^6 m/s, and Wang et al. observed an attempted leader with a low propagation velocity of 7.4×10^4 m/s.

Attempted leader develop along residual channels, and many researchers believe that attempted leader are similar to K changes and dart leader, which can be revealed by the similarity of their fast electric field waveform changes. A basic hypothesis for the cause of attempted leader extinction is that the energy of the attempted leader is not sufficient to re-ionize the channel to the surface, and thus dies midway. Shao et al. [7] believe that the initial return stroke would accumulate negative charge at a lower height from the ground, which would force the attempt leader to die out. Zhang et al. [8] believed that the appearance of the attempted leader could accumulate charge into the channel, and the initial position of the attempted leader would become a part of the next leader channel.

Both dart and attempted leader are likely in fact recoil leader, and that the main difference between them is grounding or not. Recoil leading is an electrical breakdown process that occurs in residual channels of lightning branches at high temperature and low density. Optical records of the recoil leader show that the recoil leader appears in the branching residual channel and develops towards the starting position of the branching, that is, the direction of propagation is opposite to the branch that originally formed the channel, so the recoil leader was also known as the fallback leader. Early studies of recoil leader suggested that recoil leader occur only in darkened positive leader channels and confirmed that recoil leader is bi-polar. Mazur et al. [9] observed the generation and bidirectional propagation of multiple recoil leader in the residual channel of an upward positive leader. Zhu et al. [10] believe that recoil leaders do not only appear in the residual channel of the positive polarity leader, but also may be generated in the residual channel of the negative polarity leader. Qie et al. [11] reported a bidirectional recoil leader in 2017, whose positive polar end develops along the residual channel of the negative polar leader, confirming that recoil leaders may appear in both the residual channel of the positive and negative polar leader.

Recoil leader is a bi-directional bi-polar leader, and the bi-directional leader theory was first proposed by Kasemir. Different from the source charge model proposed by Schonland earlier, the bidirectional leader theory believes that the lightning channel can be regarded as a conductor in the strong electric field of lightning cloud. Charge concentration and electric field enhancement appear at both ends of the conductor under the action of electrostatic induction, and electric breakdown process occurs when the electric field reaches a certain degree. The channel of opposite polarity takes energy from the surrounding electric field and propagates in the opposite direction, while maintaining a net charge of zero and roughly a uniform potential throughout the channel. The positive and negative ends of the bidirectional lead show asymmetry in development, and the positive end may either propagate faster or slower, or at a rate similar to that of the negative end.

The researchers have been successful record by various means to the emergence of a large number of bidirectional leader and put them into two main types: the first type of bi-directional leader began in the both sides of the metal objects, such as aircraft, dangling conductor, and the method of “altitude” in impending metal lead artificial triggered lightning. The second type of bidirectional leader is the electroless discharge process, and their formation process is summarized by Tran and Rakov [12] into four main scenarios: (1) lightning initiation process in cloud; (2) bifurcation process of lightning channel; (3) the spatial leader development process in the formation of new negative stepped leader; (4) Recoil leader type processes leading to K change, dart leader and M component process.

1.3.2 Initial Discharge Stage

The initial discharge process of classical artificially triggered lightning is similar to the natural ascending lightning caused by the top of a tall building [13]. Based on the data of manually triggered lightning in Alabama and Florida, Wang et al. believed that the geometric average duration of the initial stage was 279 ms, the geometric average of the amount of transferred charge in the initial stage was 27 C, and the average current was between 27 and 316 A, with a geometric average of 96 A. Miki et al. found that the geometric average duration of the initial stage was 305 ms, the geometric average amount of transferred charge in the initial stage was 30.4 C, and the geometric average of the average current was 99.6 A. By using the data of artificial triggered lightning in Shandong, Xiushu et al. found that the geometric mean duration of initial period was 245 ms, the geometric mean of transferred charge was 21.2 C, the geometric mean of average current was 86.7 A. Based on the data of manually triggered lightning in Guangdong, Zheng Dong et al. found that the geometric average duration of the initial stage was 347.9 ms, the geometric average of transferred charge amount in the initial stage was 45.1 C, and the geometric average of the average current was 132.5 A, slightly larger than the initial discharge parameter values of other two lightning sites. It can be seen that the overall characteristics of the initial lightning current in different regions have certain similarities.

During upward positive leader development, the rocket line is continuously heated by the initial current and melts, resulting in a sudden drop in current and a short interruption process. This current characteristic is known as the initial current change (ICV). Wang et al. found that the geometric mean value of the time interval between the slow change of current at the initial stage and the sudden drop of current was 8.6 ms, and the geometric mean value of the peak value before the current started to drop was 312 A, with the current drop time of several hundred microseconds. Then a current pulse with a rise time of about 100 μ s is generated immediately or at intervals of several milliseconds. The current pulse amplitude is usually about 1 kA. At this time, the discharge channel is re-conducted. The duration of the entire initial current change exceeds 10 ms. Biagi et al. observed with a high-speed camera of 50,000 frames per second that when the rocket line melts, due to the inhomogeneity of the rocket line, the discharge channels do not immediately brighten up, but several parts of the rocket line brighten up first until they all brighten up. Meanwhile, it was recorded that the transferred charge amount before the rocket line melts is 2.7 C. The average current in the initial stage is 59 A. After the initial discharge starts 45 ms, the rocket line begins to vaporize, and the entire rocket line vaporization process lasts about 7 ms. Rakov et al. analyzed the process related to the melting of rocket line and its replacement by air plasma channel based on fringe camera, electromagnetic field and current data, and found that the characteristics of the initial current change in the electric field waveform were V-shaped, superimposed on the electric field slope of millisecond magnitude generated by the upward positive leader. However, their current and electromagnetic fields are not measured synchronously. Olsen et al. confirmed the results of Rakov et al. and defined two

types of initial current changes of type I and type II, which had different shapes during the initial current changes, and found multiple attempted reconnection pulses with an amplitude of about 100 A before the discharge channel was re-conducted. But these attempted reconnection pulses were not optically observed. Zhang et al. analyzed 54 pre-breakdown discharge pulses generated during rocket ascent using a high-resolution VHF wideband interferometer, which were related to air breakdown at the top of the rocket. Li et al. discussed in detail the channel fracture in the initial stage and the detailed discharge process of the subsequent channel reconstruction by using VHF mapping array, electromagnetic field and high-speed camera. The channel reconstruction process is similar to the leader/return stroke sequence, while the attempted reconstruction process involves more complex discharges [14]. Understanding current cutoff and reconstruction will help us understand how natural lightning strikes occur in milliseconds or less. However, the simultaneous observation of current and electric field of initial current change is lacking.

After the initial current change, the initial continuous current pulse (ICCP) is usually generated. Wang et al. observed that the geometric mean of ICC pulse amplitude was 144 A, the geometric mean of 10–90% rise time was 528 μs , the geometric mean of half-peak width was 1 ms, the geometric mean of duration was 2.5 ms, and the geometric mean of single pulse charge transfer amount was 143 mC. The geometric mean of the pulse interval was 6.5 ms, and the geometric mean of the continuous current level prior to the ICC pulse was 127 A. Jiang et al. based on the data of artificially triggered lightning in Shandong, found that the ICC pulse amplitude was 190 A, the 10–90% rise time was 462 μs , the half-peak width was 845 μs , and the neutralization charge was 273 mC. Zheng et al. based on the data of guangdong mine initiation, found that the PULSE amplitude of ICC was 69 A, the rise time of 10–90% was 812 μs , the half-peak width was 1500 μs , and the neutralization charge was 88 mC. For the observation of natural lightning, Miki et al. observed fukui chimney in Japan and found that ICC pulse amplitude was 781 A, 10–90% rise time was 44.2 μs , half-peak width was 140.7 μs , and neutralization charge was 132 mC. Heidler et al. observed the Gaisberg tower in Austria and found that the ICC pulse amplitude was 377 A, the 10–90% rise time was 110 μs , the half-peak width was 276 μs , and the neutralization charge was 122 mC. Pichler et al. observed the Peissenberg tower in Germany and found that the PULSE amplitude of ICC was 512 A, the rise time of 10–90% was 60.9 μs , the half-peak width was 153 μs , and the neutralization charge was 111 mC. It can be seen that in natural lightning, the initial continuous current pulse amplitude is larger than that in manual lightning trigger process, while the rise time and half peak width are significantly smaller than that in manual lightning trigger process. Based on VHF interferometer, Yoshida et al. [5] found that ICC pulse may be generated by the recoil streamer entering the lightning channel at the initial stage with good electrical conductivity, or the lightning channel may be intercepted by other cloud flash channels.

1.3.3 Return Stroke Stage

The leader-return stroke process of artificially triggered lightning is similar to the process of dart leader-follow-up return return in natural lightning. Therefore, artificially triggered lightning provides a new way to understand the physical characteristics of subsequent return return channel current and close distance electromagnetic field of natural lightning, and also helps to test the return stroke model theory.

Among the parameters related to lightning discharge, lightning current is a very important physical quantity, because it directly represents the discharge process and lightning intensity, and is a key parameter in lightning protection work. The maximum moment of lightning current is the return stroke current generated in the return stroke stage, which directly determines the intensity of electromagnetic radiation. The waveform characteristics of return stroke current are also important basis for lightning protection design.

Zheng et al. summarized the waveform parameter characteristics of 142 return stroke current of artificially triggered lightning in Guangdong from 2008 to 2016, the minimum value of return current was 3.9 kA, the maximum value was 46.0 kA, and the geometric average value was 17.2 kA. Qie et al. analyzed the waveform parameters of 36 return current of artificial triggered lightning in Shandong during 2005–2011, the geometric mean of return stroke current was 12.1 kA. Fisher, Depasse, Rakov, Crawford, Uman, Schoene et al. summarized the waveform parameter characteristics of manually triggered lightning return current in Florida, USA, and the statistical results showed that The average return current is 12, 14.3, 13.3, 11.7, 13.5, 12.2 kA, 10–90% rise time is in the range of 1.4–1.9 μs , half peak width is in the range of 14.8–29.4 μs . There is a linear relationship between current rate dI/dt and peak current I . There is a strong positive correlation between the amount of transfer charge and the logarithm of current, and a relatively strong positive correlation between the action integral and the logarithm of current. Schoene et al. also found that the relationship between the peak return current and the amount of transferred charge decreases with the increase of the duration of charge transfer since the return current occurs.

The measurement of lightning electromagnetic field is not only an important basis for lightning protection design, but also plays an important role in testing the ground flash return stroke model. Miki et al. designed a set of Pockels electric field measurement equipment based on the electric-optical principle, and observed that the electric field variation presented a V-shaped structure at a very close distance of 0.1–5 m from the lightning channel. Rakov et al. analyzed the electric field waveform obtained in Florida and found that the amplitude of the leader electric field and the peak value of the return electric field were of the same order of magnitude at a close distance (tens of meters or more) to the lightning channel, and the amplitude of the leader electric field was linearly positive correlated with the peak value of the return stroke current at the bottom of the channel. Uman et al. analyzed the time differential of lightning return electric field waveforms triggered when they were 10, 14 and 30 m away from the lightning channel, and Fourier analysis results showed that

the primary frequency content of these waveforms was lower than 20 MHz. Schoene et al. introduced 28 electromagnetic waveforms and their waveform parameters that triggered lightning at distances of 15 and 30 m, and compared them with previous results. Qie et al. analyzed the electric field and current waveform of 5 artificially triggered lightning acquired in binzhou, Shandong province in summer 2005, and estimated the return stroke speed of 1.4×10^8 m/s by using the transmission line model. Le Vine et al. were the first to measure the electromagnetic field waveform of artificially triggered lightning at a distance of 5.16 km from the lightning channel. The results showed that the return electromagnetic field at this distance was basically radiation field, which was similar to the subsequent return of natural lightning, and the rise speed of triggered lightning was faster than that of natural lightning. Mallick et al. analyzed the detailed characteristics of the electric field waveform of 69 negative ground flash return strokes of 13 times of mine firing at a distance of 45 km in Florida in 2012. Wang et al. analyzed the multi-station synchronous measurement electric field waveform of 38 triggered lightning return strokes at a distance of 68–126 km from Conghua, Guangdong province in 2014, and compared it with the subsequent return stroke electric field waveform of natural lightning. Lightning location system based on waveform parameter characteristics of return stroke electric field has been widely used in power system and meteorological research [15].

Krider et al. produced the first wide-band magnetic antenna system for measuring magnetic fields caused by distant lightning. Lin et al. analyzed the electric and magnetic field waveforms generated by the first and subsequent return strokes in negative natural lightning in Florida, with a range of 1–200 km. Rakov et al. provided new insights into the lightning discharge process by using synchronous data of channel base currents and electromagnetic fields at different distances from the discharge channel. Schoene et al. further introduced the statistical characteristics of electromagnetic field and its time derivative at 30 m distance of manually triggered lightning in Florida.

Qie et al. analyzed the influence of different factors on short-range magnetic field, such as current rise time, return stroke speed, distance and peak current, by numerical method based on the data from 2005 to 2009 in the experiment of artificially triggered lightning in Shandong. Lu et al. designed a low-frequency magnetic field antenna to invert the time-varying waveform of continuous current in artificially triggered lightning, and analyzed the characteristics of magnetic field waveform at 2 m underground near the lightning channel at the initial stage of discharge.

1.3.4 Continuous Current Stage

The return stroke process is usually completed in tens of microseconds, but after the return stroke, there may still be hundreds of amperes, even up to the kA level of continuous current in the return stroke channel, the duration is usually tens to hundreds of milliseconds, accompanied by the continuous glow of the discharge channel.

Hagenguth and Anderson et al. found the current component of continuous current for the first time in the long-term lightning observation of the Empire State Building. According to the bidirectional breakdown theory, after the return is complete, the positive leader will continue to develop in the cloud, transmitting a continuous negative charge to the ground and generating a slow, long-term continuous current [16]. The amount of charge transferred by continuous current usually accounts for more than 75% of the total transferred charge. A return stroke usually releases only a few coulombs of charge, while a continuous current can release tens or more. Such lightning processes are prone to forest fires, thermal damage to metal equipment, and damage to overhead lines.

Shindo and Uman et al. analyzed that the average continuous current is about 100 A, the minimum is 30 A, and the maximum is 200 A, and the amount of transferred charge varies in the range of 10–20 C, which has been applied to the lightning protection design parameters of the International Electrotechnical Commission (IEC). Qie et al. analyzed a positive ground flash continuous current event of Chinese inland plateau, the average continuous current was about 88.2 A, the transferred charge quantity was 26.5 C in 300 ms.

The continuous current could be divided into two types according to the duration of continuous current [17]. The continuous current less than 40 ms is called short continuous current. Greater than 40 ms is called long continuous current. Rakov and Uman et al. analyzed lightning events with single and multiple returns and found that both single and multiple returns may be accompanied by a continuous current process. However, the probability of long continuous current occurring in single return lightning events is 6%, and the probability of multiple return lightning events is 49%. Moreover, for multiple return lightning events, the probability of long continuous current occurring after the first return lightning event is 1.4%, and the probability of long continuous current occurring in subsequent return lightning events is 3–15%.

Wang et al. conducted statistical analysis of negative ground flash continuous current in The Greater Hinggan Mountains. The results show that the negative ground flash with continuous current process accounts for about 27%, in which the continuous current duration of 20–40 ms has the highest probability of 23%, followed by 10–20 ms, accounting for about 12%, and the probability of 80–100 ms and 40–60 ms is 11 and 10%, respectively. The average duration of continuous current is 127.4 ms, and the maximum duration is over 400 ms. It can be seen that the probability and duration of continuous current occurrence are affected by different regions.

Fisher et al. analyzed the data of triggered lightning in Florida and found that when the continuous current lasts for more than 10 ms, the current waveform presents different characteristics, which can be divided into four types: the first type is accompanied by superimposed current pulses after the return stroke, which show exponential attenuation; In the second type, a smooth attenuation peak is followed by a superimposed current pulse after the return stroke; The third is accompanied by a current pulse after the return; The fourth type, after the return stroke, is followed by a steady stasis period with no significant pulse activity, followed by the superimposed current pulses [18]. The first and second categories are the most common.

During the continuous current period, there is often an obvious current pulse activity, which corresponds to the sudden brightening of discharge channel and abrupt change of electric field. This process is called M component (similar to ICC pulse). Thottappillil et al. found that the amplitude of the M component current of artificially triggered lightning was 100–200 A, the rise time was 300–500 μs , and the transfer charge was 100–200 mC. Jiang et al. obtained, based on the statistics of manually triggered lightning data in Shandong, that the current amplitude of M component is about 400 A, the rise time of 10–90% is 207 μs , the half-peak width is 267 μs , and the transferred charge is 190 mC. Zheng et al. obtained from the analysis of artificially triggered lightning data in Guangdong that the amplitude of M component current was 195 A, the rise time of 10–90% was 379 μs , the half-peak width was 638 μs , and the transfer charge amount was 107 mC. For the observation of natural lightning, the observation results of Fukui Chimney in Japan, Gaisberg Tower in Austria and Peissenberg tower in Germany showed that the current amplitude of M component was 274–654 A, and the rise time of 10–90% was 37.4–236 μs . The half-peak width is 124.8–476 μs , and the transfer charge is 137–167 mC. It can be seen that the M component parameters are very similar to ICC pulses, and it is speculated that they have similar physical processes. In terms of current amplitude, the M component and ICC pulse are obviously smaller than the return current pulse. In terms of time parameters, the rise time and half peak width of M component and ICC pulse are much larger than those of return current pulse.

By analyzing the data of artificial triggered lightning in Shandong, Qie et al. found RM pulse, which had the characteristics of return stroke pulse and M component pulse, with large current amplitude, which could reach the order of peak of return stroke current. They hypothesized that the generation of RM pulses was related to the bifurcation development of positive leads within the cloud. When one channel continues to glow and the other channel cuts off, the recoil streamer enters such a discharge grounding channel, and the two simultaneous effects may produce RM pulses [19]. In natural lightning, some M components are not weaker than the return stroke, which may lead to misjudgment of the lightning location system.

References

1. Newman MM, Stahmann JR, Robb JD, et al. Triggered lightning strokes at very close range[J]. *Journal of Geophysical Research Atmospheres*, 1967, 72(18):4761–4764.
2. Rakov VA, Uman MA, Raizer YP. Lightning: physics and effects[J]. *Physics Today*, 2004, 57:63–64.
3. Li Jun, LV Weitao, ZHANG Yijun, et al. A multi-bifurcation and multi-ground air-triggered lightning process [J]. *Journal of Applied Meteorology*, 2010(01):95–100. (in Chinese)
4. Qie XS, Zhang QL, Zhou YJ, et al. Artificially triggered lightning and its characteristic discharge parameters in two severe thunderstorms[J]. *Science in China Series D*, 2007, 50(8):1241–1250.
5. Yoshida S. Three-dimensional imaging of upward positive leaders in triggered lightning using VHF broadband digital interferometers[J]. *Geophysical Research Letters*, 2010.

6. Rhodes CT, Shao XM, Krehbiel PR. et al. Observations of lightning phenomena using radio interferometry[J]. *Journal of Geophysical Research*, 1994, 99(D6):13059.
7. Shao XM, Krehbiel PR, Thomas RJ. et al. Radio interferometric observations of cloud-to-ground lightning phenomena in Florida[J]. *Journal of Geophysical Research*, 1995, 100(D2):2749.
8. Zhang G, Zhao Y, Qie X. et al. Observation and study on the whole process of cloud-to-ground lightning using narrowband radio interferometer[J]. *Science in China Series D: Earth Sciences*, 2008, 51(5):694–708.
9. Mazur V, Ruhnke L H, Warner T A. et al. Recoil leader formation and development[J]. *Journal of Electrostatics*, 2013, 71(4):763–768.
10. Zhu Y, Rakov V A, Tran MD. Et al. A subsequent positive stroke developing in the channel of preceding negative stroke and containing bipolar continuing current[C]. *IEEE*, 2016.
11. Qie X, Pu Y, Jiang R. et al. Bidirectional leader development in a preexisting channel as observed in rocket-triggered lightning flashes: bileader in a preexisting channel[J]. *Journal of Geophysical Research: Atmospheres*, 2017, 122(2):586–599.
12. Tran MD, Rakov VA. Initiation and propagation of cloud-to-ground lightning observed with a high-speed video camera[J]. *Scientific Reports*, 2016, 6(1):39521.
13. Zhou H, Rakov V A, Diendor Fe R G, et al. A study of different modes of charge transfer to ground in upward lightning[J]. *Journal of Atmospheric and Solar-Terrestrial Physics*, 2015, 125-126:38–49.
14. Li S, Qiu S, Shi L, et al. Observations of the wire destruction and plasma channel reestablishment process during the initial stage of triggered lightning[J]. *Geophysical Research Letters*, 2020, 47(3).
15. Cai L, Zou X, Wang J, et al. The Foshan Total Lightning Location System in China and its initial operation results[J]. *Atmosphere*, 2019, 10(3).
16. Hagenguth JH, Anderson JG. Lighting to the Empire building[J]. Part III. *AIEE*, 71:641–649.
17. Kitagawa N, Brook M, Workman EJ. Continuing currents in cloud-to-ground lightning discharges[J]. *Journal of Geophysical Research*, 1962, 67(2):637–647.
18. Fisher RJ, Schnetzer GH, Thottappillil R, et al. Parameters of triggered-lightning flashes in Florida and Alabama[J]. *Journal of Geophysical Research Atmospheres*, 1993, 98(D12):22887–22902.
19. Qie XS, Jiang RB, Wang CX, et al. Simultaneously measured current, luminosity, and electric field pulses in a rocket-triggered lightning flash[J]. *Journal of Geophysical Research-Atmospheres*, 2011, 116(D11):1–11.

Chapter 2

Characteristics of Lightning Current of Rocket-Triggered Lightning



In the case of negative ambient electric field, traditional rocket-triggered lightning mainly includes upward positive leader (UPL), initial continuous current (ICC), one or more downward-leader-upward-return-stroke sequences, continuous current and M component, etc. Among them, the upward positive leader and continuous current constitute the initial discharge process (IS). The initial discharge process lasts tens to hundreds of milliseconds, and the current pulse superimposed on the initial continuous current is called the ICC pulse, similar to the M component. M component pulse overlap the continuing current. Before the continuous development of the upward leader begins, the attempted breakdown at the top end of the wire causes the sequence of precursor pulses.

2.1 IS Currents

2.1.1 Parameters of IS Current

18 TLFs with complete current recording information, including 17 classical TLFs and an altitude TLF, were statistically analyzed [1]. The Rogowski coil and coaxial shunt were used as lightning current measuring equipment. In the control room, the currents were synchronously sampled in two channels with small (± 2 kA) and large (± 50 kA) measurement ranges via a multi-channel high-speed digital oscilloscope (DL850E). The oscilloscope sampling rate was 5 MHz in 2018, and it was improved to 50 MHz in 2019. The recording length was 2 s. All classical TLFs were successfully conducted into the distribution line. A total of 70 RSs were recorded in 17 classical TLFs and 8 RSs were recorded in one altitude TLF judged by electric field. In 17 classical TLFs, 4 classical TLFs only contained IS, without RS. The information of these lightning discharges is given in Table 2.1.

Table 2.1 List triggered-lightning striking to distribution line

| Flash number | Time | Return stroke number | M component number |
|---------------|------------------|----------------------|--------------------|
| F201806261150 | 26-June 11:50:34 | 1 | 0 |
| F201807021442 | 2-July 14:42:58 | 3 | 1 |
| F201807071631 | 7-July 16:31:02 | 0 | 0 |
| F201807261411 | 26-July 14:11:24 | 13 | 22 |
| F201807261414 | 26-July 14:14:24 | 1 | 4 |
| F201807261417 | 26-July 14:17:48 | 0 | 0 |
| F201906051620 | 5-June 16:20:28 | 4 | 28 |
| F201906051625 | 5-June 16:25:34 | 0 | 0 |
| F201906061414 | 6-June 14:14:24 | 5 | 2 |
| F201906111242 | 11-June 12:42:28 | 9 | 15 |
| F201906111303 | 11-June 13:03:43 | 0 | 0 |
| F201906111307 | 11-June 13:07:17 | 3 | 0 |
| F201906111315 | 11-June 13:15:33 | 4 | 5 |
| F201906301713 | 30-June 17:13:13 | 9 | 13 |
| F201906301716 | 30-June 17:16:17 | 5 | 1 |
| F201907021512 | 2-July 15:12:36 | 2 | 0 |
| F201907021521 | 2-July 15:21:23 | 11 | 15 |
| F201907071802 | 7-July 18:02:59 | 8 | 9 |

Cai et al. [2] analyzed the current parameters of the IS stage. The main parameters of the IS examined in this study include duration (D), maximum current, average current, charge transfer (Q), and the action integral (AI). For one of the TLFs, F201906051620, the start position of the IS current could not be identified precisely; therefore, 16 IS current samples in total were counted in the study. Two examples of the IS current waveforms were shown in Fig. 2.1.

The IS current waveforms can be divided into two categories: ISs with silence period (4/16), as shown in Fig. 2.1b, and ISs without silence period (12/16). The GMs of duration, maximum current, average current, charge transfer, and the action integral of ISs with silence period are 168.0 ms, 1.0 kA, 28.5 A, 4.8 C and 220.0 A²s, respectively. And the GMs for those ISs without silence period are 305.4 ms, 0.6 kA, 85.9 A, 26.2 C and 3701.1 A²s, respectively. It is found that the ISs without silence period show longer duration, larger average current, charge transfer, and the action integral than those with silence period. For those TLFs of ISs without silence period, only one (1/16) TLF had no return stroke. However, for those TLFs of ISs with silence period, three (3/4) TLFs had no return stroke.

Overall, the IS current parameters and their descriptive statistics are shown in Fig. 2.2. The GM duration of 263.0 ms was slightly lower than the GM of 279 ms reported by Wang et al. [3] and the GM of 305 ms reported by Miki et al. [4] in their study of TLFs in Florida and lower than the AM of 399.5 ms and the GM of

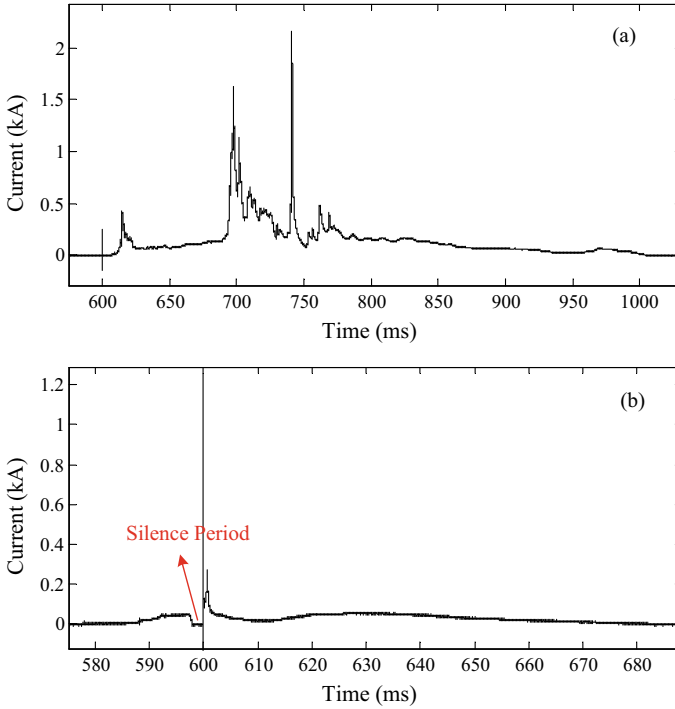


Fig. 2.1 Two examples of the IS current waveforms

347.9 ms reported by Zheng et al. [5] in GCOELD. However, the GM duration was slightly higher than the GM of 245 ms reported by Qie et al. [6] in Shandong. The AM maximum current of 0.9 kA and the GM of 0.7 kA were all less than the AM of 2.7 kA and the GM of 1.3 kA in GCOELD. For the average current, the GM (65.2 A) was smaller than the value of 96 A recorded by Wang et al. [3], the value of 99.6 A recorded by Miki et al. [4] for the triggered lightning in Florida, the value of 132.5 A in GCOELD and the value of 86.7 A in Shandong. The values of charge transfer in the IS were less than 100 C. The GM of the charge transfer was 17.2 C, which was less than the values of 27, 30.4, 45.1 and 21.2 C reported by Wang et al. [3], Miki et al. [4], Zheng et al. [5], and Qie et al. [6]. As for the action integral, the GM of $1.8 \times 10^3 \text{ A}^2\text{s}$ was less than those (8.5×10^3 and $10.0 \times 10^3 \text{ A}^2\text{s}$) reported by Miki et al. [4] and Zheng et al. [5].

The correlations between IS current parameters are shown in Fig. 2.3. The duration and charge transfer show moderate correlation. We did linear fitting and power function fitting and built the regression equation of $Q = -4.768 + 0.09D$, with $R^2 = 0.57$ and $Q = 0.018D^{1.243}$, with $R^2 = 0.57$, respectively. However, Zheng et al. [5] reported exponential correlation between the duration and charge transfer and built the regression equation of $Q = 13.511\exp(0.003D)$, with $R^2 = 0.58$. The moderate

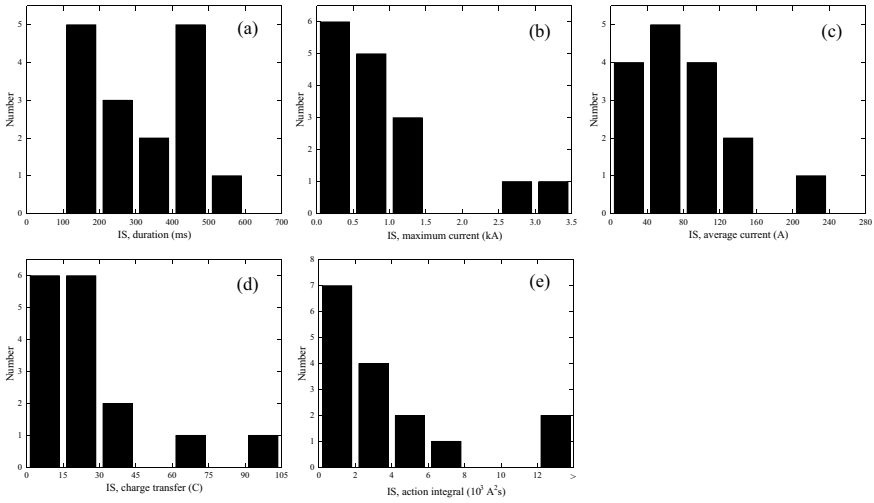


Fig. 2.2 The IS current parameters and their descriptive statistics

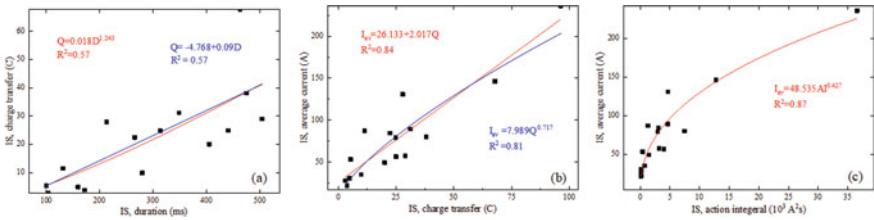


Fig. 2.3 The correlations between IS current parameters

correlation between IS duration and IS charge transfer (correlation coefficient $R^2 = 0.7$) was also suggested by Wang et al. [3] with linear fitting.

Meanwhile, we also did linear fitting and power function fitting between the average current and charge transfer. The regression equation are $I_{av} = 26.133 + 2.017D$, with $R^2 = 0.84$ and $I_{av} = 7.989Q^{0.717}$, with $R^2 = 0.81$, respectively. Zheng et al. [5] reported the regression equation of $I_{av} = 23.641Q^{0.441}$, with $R^2 = 0.53$. Wang et al. [3] also reported the linear correlation between IS average current and IS charge transfer (correlation coefficient $R^2 = 0.8$).

An excellent power function relation describes the correlation between the average current and action integral. The regression equation is $I_{av} = 48.535AI^{0.427}$, with $R^2 = 0.87$. Zheng et al. [5] also reported the regression equation of $I_{av} = 57.326AI^{0.355}$, with $R^2 = 0.89$.